BL2B

Measurement of Kinetic Energies of Fragments Produced by the Photodissociation of C_{70} Using Velocity Map Imaging

H. Katayanagi[1,2] and K. Mitsuke[1,2]

[1]*Dept. of Photo-Molecular Science, Institute for Molecular Science, Okazaki 444-8585, Japan*

[2]*Graduate University for Advanced Studies, Okazaki 444-8585, Japan*

We have developed a photofragment imaging spectrometer suitable for synchrotron radiation excitation of gaseous molecules of refractory materials [1]. Using this apparatus we have observed the scattering distributions of the fragments produced by the photodissociation of C_{60} [2]. We have recently performed a same kind of experiment using C_{70} as a sample [3]. This series of the experiments on the fullerenes is the first attempt of applying our imaging technique to the energetics and dynamics of comprehensive decay chain starting from large clusters.

The experiments were performed at BL2B in UVSOR. Fullerene (C_{70}) powder was loaded in a quartz tube and heated up by an electric heater in vacuum. The C_{70} vapor passed through two apertures and reached the ionization region, where the C_{70} molecular beam (x axis) intersected the monochromatized synchrotron radiation (y axis) at right angles. Ions produced at the ionization region were extracted by a velocity map imaging electrode assembly and projected along z axis on to a position sensitive detector (PSD). Photoelectrons were extracted to the opposite direction to the ions and detected by a microchannel plate detector. Time of flight (t) and arrival position (x, y) of ions on the PSD were recorded using the signal of photoelectrons as a start trigger. Three-dimensional (3D) lists of data, (x, y, t), were thus obtained. Integration of the 3D listdata with respect to x, 2D y-t distributions (y-t maps) were obtained (not shown here, see Ref. 3). Distributions along y-direction on the y-t map with limited t ranges which correspond to mass-to-charge ratios (m/z) of fragments were then extracted. The y-distribution of a fragment is 1D projection of 3D velocity distribution and is converted to a translational temperature.

The translational temperatures were converted to the kinetic energy release (KER) in each C_2 ejection step such as $C_{70-2n+2} \rightarrow C_{70-2n} + C_2$. The values of KER at the nth step of the reaction are shown in Fig. 1. The values of KER are found to be approximately 0.4 eV at 110 eV except for the n=5 (C_{60}^{2+} production) step. The KER for the n=5 step is exceptionally smaller than those for the n=1～4 steps.

We performed an analysis based on the finite-heat-bath theory to interpret the above KER values. The analysis predicts minimum cluster sizes which are detectable in these photon energies and the values of KER for these clusters. Figure 2 shows the theoretical (filled symbols) and experimental (open symbols) values of KER. The theoretical values agreed with the experimental values if we assume the excess energy in the parent ion is smaller by 15 eV than the maximum available energy. This shift can be ascribable to the energy of photoelectrons. In Fig. 2 we can recognize that C_{60}^{2+} fragments are produced with small kinetic energy release, in contradiction to theoretical predictions. This may suggest that other fragmentation mechanisms are involved in the formation of C_{60}^{2+}.

We are now improving this apparatus to be applicable to functional materials such as carbon nanotubes and ionic liquids, which are indispensable in the development of renewable energy technology.

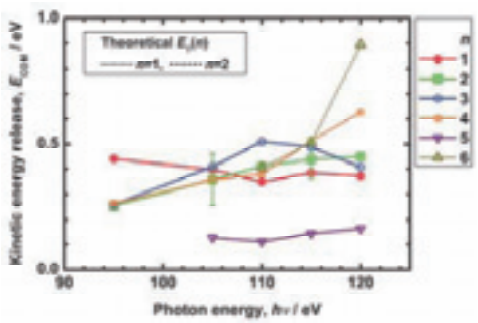

Fig. 1. Excitation photon energy dependence of average KER generated at the n-th reaction step to produce C_{70-2n}^{2+}. Error bars show the uncertainty caused in the fitting procedure.

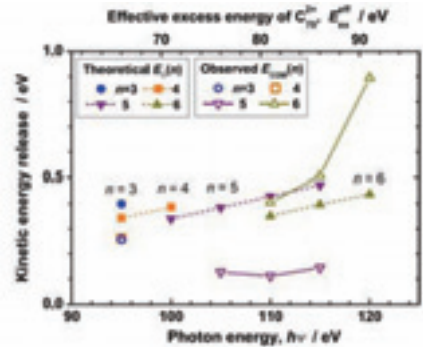

Fig. 2. Theoretical (filled symbols) and experimental (open symbols) kinetic energy release generated at the nth reaction step.

[1] Md. S. I. Prodhan *et al.*, Chem. Phys. Lett. **469** (2009) 19.

[2] H. Katayanagi and K Mitsuke, J. Chem. Phys. **133** (2010) 081101.

[3] H. Katayanagi and K. Mitsuke, J. Chem. Phys. **135** (2011) 144307.

BL2B

Dissociative Photoionization of Perfluorocyclobutane Studied by Mass-Resolved Photoion Imaging

K. Okada[1], T. Nakashima[1], Y. Fukuoka[1], A. Suemitsu[1], H. Katayanagi[2, 3] and K. Mitsuke[2, 3]

[1]*Department of Chemistry, Hiroshima University, Higashi-Hiroshima 739-8526, Japan*

[2]*Institute for Molecular Science, Okazaki 444-8585, Japan*

[3]*School of Physical Sciences, The Graduate University for Advanced Studies (SOKENDAI), Okazaki 444-8585, Japan*

Molecular photoionization and ionic fragmentation processes are of fundamental importance in the upper-atmospheric chemistry and plasma physics. Perfluorocyclobutane (*c*-C_4F_8) is extensively used as a reagent for dry etching of semiconductors. The accurate knowledge of its chemical processes is required to evaluate the role in the upper atmosphere. In our previous study [1] we have reported yield spectra of the fragment ions of *c*-C_4F_8 in the photon energy range of 25–170 eV. Measurements by use of a photoelectron–photoion–photoion coincidence (PEPIPICO) technique were also conducted to study the breakdown pathways. From coincidence islands found in the PEPIPICO spectra, several deferred charge separation processes were identified.

This study is a continuation of the previous report. We particularly focus on the kinetic energy of CF_2^+ to get more insight concerning the dissociation energetics of the *c*-C_4F_8 system.

The experiments have been performed on the beamline BL2B at the UVSOR facility. The experimental setup has been described in a previous paper [1]. Arrangement of the electrostatic lens system employed in this study was described in Ref. [2]. The photoions traveling through the flight tube were detected with a position sensitive detector (Quantar Technology, 3394A). Position signals of the photoion arrival were fed into a multi-parameter data acquisition system (FAST ComTec, MPA) together with photoelectron signals for triggering the real time clock. The list of a data set (*x*,*y*,*t*) was stored in a personal computer as a list-mode file. The data were acquired at the excitation energies of 40.0, 55.0, 60.0 and 80.0 eV. A series of time-of-flight (TOF) spectra were also measured separately while scanning the photon energy in the range of 35–55 eV.

The upper panel of Fig. 1 depicts a typical *y*–*t* map of the photofragment ions, measured at the excitation energy of 40.0 eV. It is obtained by integrating the (*x*,*y*,*t*) data with respect to *x*. The ion counts are displayed in color. Intense bar-shaped spots with different lengths can be found in the map. The length reflects the departing velocity of each fragment ion. Summation of the counts of the map over all *y* yields a familiar TOF spectrum. The resulting spectrum is given in the lower panel of Fig. 1, being in perfect agreement with the previous measurement [1].

We found that for the CF_2^+ ion the bar length depends on the photon energy. The velocity distribution of the ion was derived from the signal counts of the *y*–*t* map over the time range corresponding to the CF_2^+ peak. The kinetic energy at the half-maximum intensity is 1.7 times as high in the 60.0-eV data as in the 40.0-eV data. This result can be qualitatively understood in such a way that with increasing the photon energy the CF_2^+ ion is released with higher kinetic energy due to a lighter ion forming at an early step of the fragmentation mechanism.

More detailed analysis of the imaging data is in progress and the results will be published in the near future.

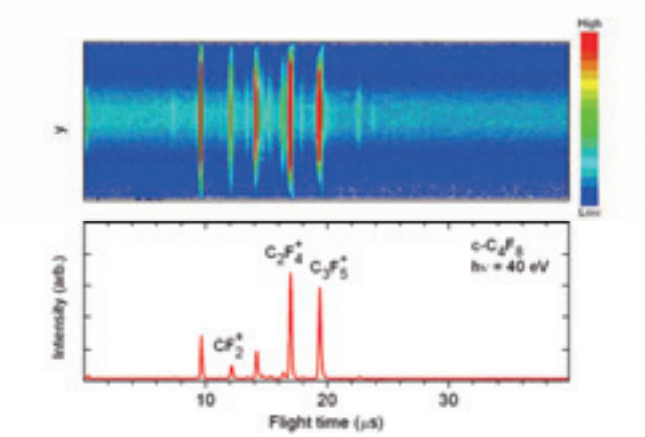

Fig. 1. A typical *y*–*t* map of the photofragment ions of *c*-C_4F_8 acquired at 40.0 eV (the upper panel) and its corresponding TOF spectrum (the lower panel). On the *y*–*t* map the signal counts are plotted as a function of the arrival time *t* and the *y* coordinate of the position on the ion detector. Summation of the counts over the whole *y* gives the TOF spectrum.

[1] K. Okada, T. Nakashima, M. Sakai, A. Suemitsu, C. Huang, H. Yagi, H. Katayanagi, K. Mitsuke and K. Tabayashi, J. Phys. Conf. Ser. **288** (2011) 012021.

[2] H. Katayanagi and K. Mitsuke, J. Chem. Phys. **133** (2010) 081101.

BL3U

Development of a Novel Nozzle for Probing Large Molecules in Vacuum Chamber by Photoelectron Spectroscopy

T. Gejo[1], T. Tajiri[1], K. Honma[1], M. Nagasaka[2] and N. Kosugi[2]
[1]*Univ. of Hyogo, Koto 3-2-1, Kamigori-cho, Hyogo 678-1205, Japan*
[2]*Institute for Molecular Science, Okazaki 444-8585, Japan*

The liquid water has been regarded as fundamental material and has been investigated for many years. Particularly interest is the hydrogen network in liquid water, which were investigated by many spectroscopic studies. Since then, many models have been proposed. Recently, in order to investigate the electronic states of liquid water with hydrogen networks, photoelectron spectroscopy and soft x-ray emission spectra have been investigated. To obtain those spectra, liquid phase in vacuum chamber is necessary. Therefore, liquid water beam technique [1] has been employed.

For this experimental, we have developed the device that utilizes ultrasonic atomization to produce a dense aerosol microdroplet of water. The ultrasonic atomization technique has been used for generate the microdroplets in mist: The size of liquid droplets was distributed around the micrometer scale. Therefore one can achieve micro droplet of liquid water in vacuum chamber by the injecting them directly.

The experiments were carried out on the undulator beamline BL3U at the UVSOR facility in IMS. The experimental set-up consists of three parts: a mist generation part, a transportation part and a nozzle. The microdroplets are generated via ultrasonic atomization. Ultrasonic oscillators (HM2412, Honda Electronics Co., Ltd) operating at 2.4 MHz were installed at the bottom of the water bath. The micro droplet were carried by Ar and pumped out to obtain a stable stream. Figure 1 shows the picture of the stream of mist. A 0.5 mm diameter nozzle hole has been placed just before pumping system and the leaked microdroplet go into the vacuum chamber. After the skimmer, 100 eV VUV photons have been radiated to the microdroplets and the photoelectron spectra has been measured by SIENTA installed.

The water molecule has C_{2v} symmetry with electronic configuration $1a_1 2a_1 1b_2 3a_1 1b_1$. $1a_1$ and $2a_1$ orbitals correspond to the oxygen 1s and 2s orbitals. $1b_1$ and $3a_1$ valence orbitals are mainly responsible for the O-H bond. The $1b_1$ valence orbital is the lone pair orbital with almost pure O 2p character.

Figure 2 shows the photoelectron spectra of water when the ultrasonic atomization apparatus was on and off. Three major peaks arise from $1b_2$, $3a_1$ and $1b_1$ electronic states. Although a small peak due to large cluster of water can be found at 87 eV kinetic energy region, two spectra are almost identical, which suggests that the generation of microdroplets was quite few in comparison with the water molecule. This is presumably due to low conductance of the nozzle, which prevent the microdroplets to pass without condensation.

We are planning a modified nozzle, in which pulsed valve with high conductance and high repetition rate is used.

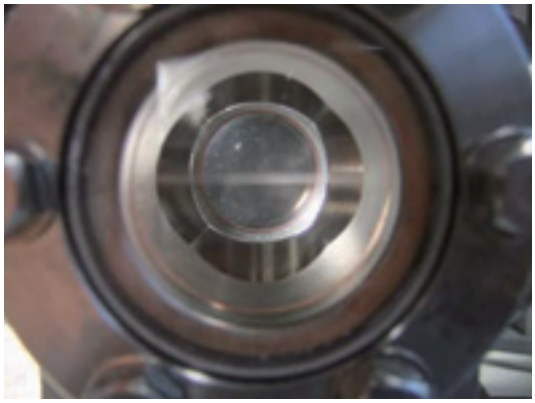

Fig. 1. The picture of mist stream of microdroplets in the view port chamber.

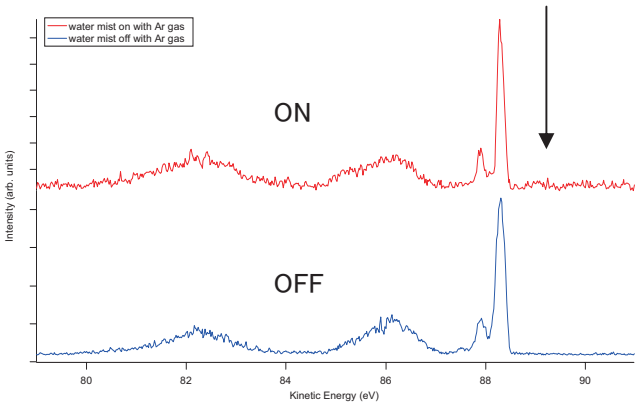

Fig. 2. The photoelectron spectra of water when the ultrasonic atomization is on and off. An arrow shows the peak position due to clusters or microdroplets.

[1] B. Winter *et al*., J. Phys. Chem. A **108** (2004) 2625.

BL3U

Local Structures of Methanol-Water Binary Solutions. I. Oxygen K-Edge Soft X-Ray Absorption Spectra

M. Nagasaka and N. Kosugi
Institute for Molecular Science, Myodaiji, Okazaki 444-8585, Japan

A water molecule has two hydrogen-accepting ('acceptor') and hydrogen-donating ('donor') sites, and liquid water forms three dimensional hydrogen bonding networks. On the other hand, a methanol molecule has one donor and acceptor sites due to a hydrophobic methyl group, and liquid methanol forms one or two dimensional hydrogen bonding networks, such as chains and rings of 6-8 methanol molecules [1]. It is known that methanol-water binary solution shows three dimensional cluster formations by interactions between water and methanol molecules [2]. But the local structures of the methanol-water mixtures are still unknown. X-ray absorption spectroscopy (XAS) is a promising method to investigate the local structure of liquid. Recently, we have developed a liquid cell for the measurements of XAS in a transmission mode [3]. In this work, the local structures of the methanol-water binary solutions at different concentrations were studied by using oxygen K-edge XAS.

The experiments were performed at BL3U. The liquid thin layer was sandwiched between two 100 nm-thick Si_3N_4 membranes (NTT AT Co.). The thickness of the liquid layer was optimized from 50 to 1000 nm by changing the He backpressure [3]. The photon energy was calibrated by the oxygen 1s – π* peak (530.8 eV) of O_2 gas mixture in He.

Figure 1 shows oxygen K-edge XAS spectra of the methanol-water solutions at different concentrations. The previous work observed the peak around 532 eV in the methanol-water mixtures [4], but it is not observed in our measurements. The pre-edge peak (535 eV) corresponds to a transition from oxygen 1s to $4a_1$* unoccupied orbital, which is mainly distributed at the oxygen atom in the water molecule, and reflect the interaction in the hydrogen bonding [5]. The intensities of the pre-edge peaks decrease with the higher mixing ratio of water. The isosbestic points are observed in the pre-edge region, which mean only the contributions of the liquid methanol and water in the XAS spectra. In order to confirm this result, the intensities of the pre-edge regions are plotted with the different concentrations, as shown in Fig. 2. We confirmed that the intensities of the pre-edge regions decrease almost linearly by increasing the mixing ratio of water. It means the interactions around the oxygen atoms in the hydrogen bonding networks are not changed at different concentrations of the methanol-water mixtures. These results suggested that the hydrogen bonding of the CH_3OH-H_2O pair is nearly the same as that of both the H_2O-H_2O and CH_3OH-CH_3OH pairs.

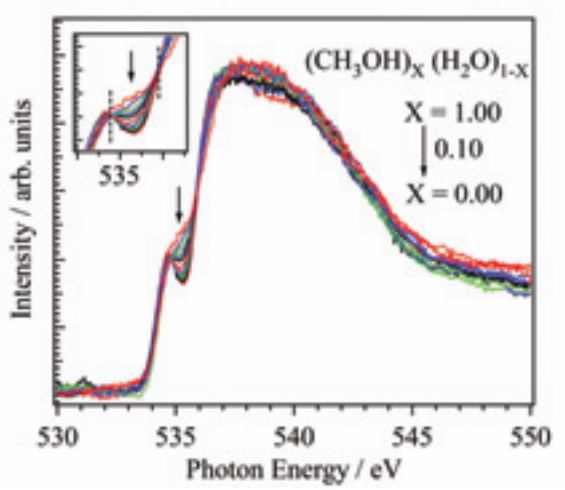

Fig. 1. Oxygen K-edge XAS spectra of the methanol-water binary solutions at the different concentrations at 25 ºC. The mixing ratio of water in the solution is increased along indicated arrows. The inset shows the isosbestic points (dashed lines) in the pre-edge region.

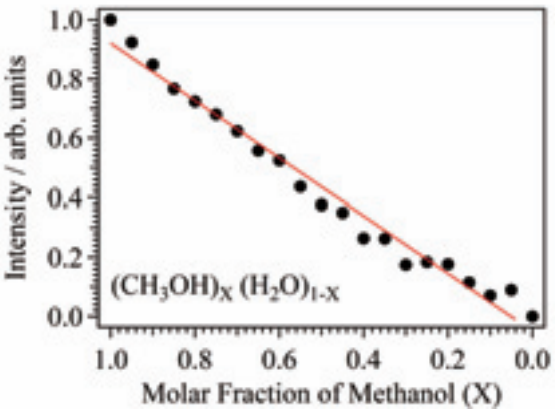

Fig. 2. Intensities of the pre-edge regions as a function of molar fraction of methanol (X) in the methanol-water mixtures $(CH_3OH)_X(H_2O)_{1-X}$. The intensities of methanol and water are normalized to one and zero, respectively.

[1] S. Sarkar and R. N. Joarder, J. Chem. Phys. **99** (1993) 2032.
[2] S. Dixit *et al*., Nature **416** (2002) 829.
[3] M. Nagasaka *et al*., J. Electron Spectrosc. Relat. Phenom. **177** (2010) 130.
[4] J.-H. Guo *et al*., Phys. Rev. Lett. **91** (2003) 157401.
[5] Ph. Wernet *et al*., Science **304** (2004) 995.

BL3U

Local Structures of Methanol-Water Binary Solutions. II. Carbon K-Edge Soft X-Ray Absorption Spectra

M. Nagasaka and N. Kosugi
Institute for Molecular Science, Myodaiji, Okazaki 444-8585, Japan

Oxygen K-edge X-ray absorption spectroscopy (XAS) of methanol-water binary solutions has revealed that hydrogen bonding is not changed at different concentrations [1]. On the other hand, the neutron diffraction studies suggested the formations of three dimensional clusters by interactions between water and methanol molecules [2]. In this work, we have measured carbon K-edge XAS spectra of the methanol-water binary solutions at different concentrations to investigate not only the hydrogen bonding but also the interactions between the methyl groups in the methanol molecules.

The experiments were performed at BL3U. The details of the experimental setups were described previously [3]. The photon energy was calibrated by the first peak (287.96 eV) of methanol gas mixture in He.

Figure 1 shows the carbon K-edge XAS spectra of the methanol-water binary solutions at the different concentrations. Because the carbon atom is contained only in the methanol molecule, carbon K-edge XAS spectra include the core excitations of the methanol molecules. The peak around 288.5 eV is mainly distributed at the hydroxyl group in the methanol molecule, and reflects the hydrogen bonding. The intensity of this peak is not changed so much at different concentrations. It is consistent with the result of the oxygen K-edge XAS, in which the hydrogen bonding is not changed irrespective of the mixing ratios [1]. On the other hand, the peak around 290 eV is mainly distributed at the methyl group in the methanol molecules. This peak is shifted to the higher photon energy by increasing the mixing ratio of water. It means that the methyl groups approach with each other and the interaction between the methyl groups increase. Liquid methanol forms chains or rings of 6-8 methanol molecules [4], and the methyl groups are apart from each other. When the water molecules join the hydrogen bonding networks, three dimensional mixed clusters are formed in the solution, and the distance between the methyl groups becomes small. The intensities of the valleys around 289 eV decrease by the higher photon energy shifts of the peak around 290 eV. Figure 2 shows the intensities of these valleys at the different mixing ratios. The intensities are changed nonlinearly, and are able to separate three regions. The intensities are not changed so much in the region I, where the mixing ratio of water is below 25 %. The intensity suddenly decrease at 25 %, and the slow decrease is continued (II). When the mixing ratio of water exceeds above 70 %, the intensity decrease becomes fast (III). The different growth mechanism of the mixed methanol-water clusters occurs at the different concentrations.

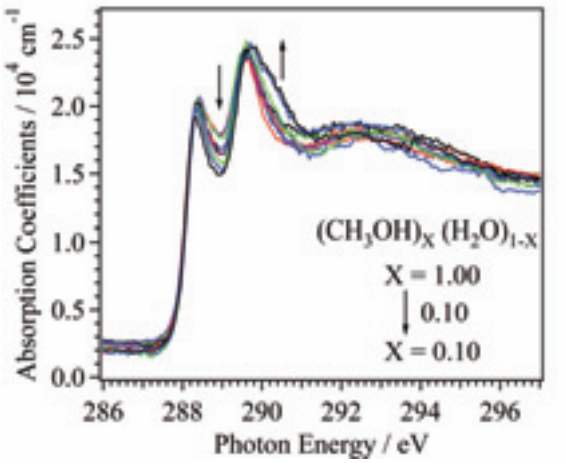

Fig. 1. Carbon K-edge XAS spectra of the methanol-water solutions at different concentrations at 25 ºC. The mixing ratio of water in the solution is increased along indicated arrows.

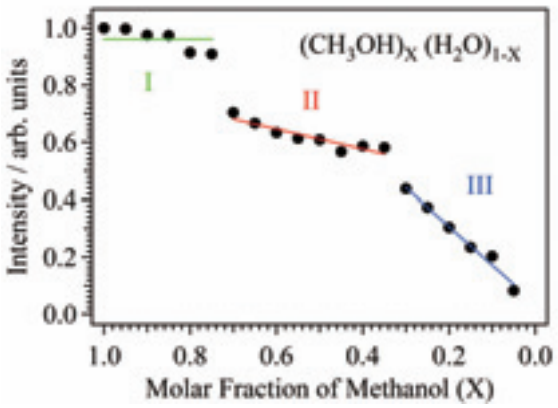

Fig. 2. Intensities of the valleys around 289 eV as a function of molar fraction of methanol (X) in the methanol-water mixtures $(CH_3OH)_X(H_2O)_{1-X}$. The intensities of methanol and water are normalized to one and zero, respectively. Three characteristic regions are found at the different molar fractions.

[1] M. Nagasaka and N. Kosugi, in this volume.
[2] S. Dixit *et al*., Nature **416** (2002) 829.
[3] M. Nagasaka *et al*., J. Electron Spectrosc. Relat. Phenom. **177** (2010) 130.
[4] S. Sarkar and R. N. Joarder, J. Chem. Phys. **99** (1993) 2032.

Absorption Spectra of L-Alanyl-L-Alanine Film from 3 eV to 250 eV

M. Iwai[1], Y. Izumi[2,*], Y. Tanigawa[2], S. Takahara[1], K. Sugiki[2] and K. Nakagawa[1,2]
[1]*Faculty of Human Development, Kobe University, Kobe 657-8501, Japan*
[2]*Graduate school of Human Development and Environment, Kobe University, Kobe 657-8501, Japan*

Absorption spectra of thin films of L-alanyl-L-alanine $C_6H_{12}N_2O_3$ were measured at the photon energy region from 3 eV to 250 eV and discussed in comparison with that of L-alanine.

Powder of L-alanyl-L-alanine was purchased from SIGMA Chemical Company. Thin films of L-alanyl-L-alanine were prepared with vacuum evaporation technique in which heater temperature was set at about 370 K. Collodion films and SiO_2 plates were used as substrate.

Spectral measurement was carried out at the beamlines 3B, 5B and 7B. Photon energy region used for measurements were 3.5 to 37 eV at BL3B and BL7B and 30 to 250 eV at BL5B. Optical density $OD(E)$ was obtained as a function of photon energy E for various samples with different thickness because magnitude of OD(E) around 20 eV was one order larger than that around 90 eV or at higher energies.

Values of absorption cross section $\sigma(E)$ was calibrated around 7 eV for thick films evaporated on SiO_2 substrate, of which $\sigma(E)$ was directly determined by high performance liquid chromatography (HPLC) technique for water solution of the evaporated film.

Because we calibrated the absolute values of $\sigma(E)$ around 7 eV where σ was one order smaller than that around 20 eV, we thought that obtained $\sigma(E)$ values might be erroneous. Thus we used the Tohmas-Reihe-Kuhn sum rule [1] of oscillator strength distribution $df(E)/dE$ in order to calibrate our values of $\sigma(E)$,

$$\int_{E_1}^{E_2} \frac{df(E)}{dE} dE = N_e \quad ,$$

where, N_e is the number of electrons responsible to the optical transition within the photon energy region from E_1 to E_2 . The relation between $\sigma(E)$ and $df(E)/dE$ is known to be

$$\sigma(E)[\mathrm{Mb}] = 1.098 \times 10^2 \cdot \frac{\mathrm{d}\, f(E)}{\mathrm{d}E} [\mathrm{eV}^{-1}] \quad .$$

Since the integration of df/dE yielded the value of N_e to be 84 which is larger than the real number N_e=64, we finally calibrated the $\sigma(E)$ to be multiplied 64/84=0.76.

The calibrated values of $\sigma(E)$ were plotted in the curve A in Fig. 1. In the figure curve B is the $\sigma(E)$ of atomic mixture 6C+12H+2N+3O calculated with the atomic absorption coefficients compiled by Henke[3].

Form the comparison of the curve A , B and C, we can point out following;

(1) Above 30 or 40 eV, experimental spectrum (curve A) is well reproduced by the atomic mixture model (curve B), which means that at higher energies, nature of optical absorption is similar with the atomic mixture.

(2) At lower photon energy region than 30 eV, optical spectrum is of molecular natures.

(3) Clear difference in optical absorption spectrum of L-alanyl-L-alanine appears at 6.3 eV at which energy the peptide bond was reported. No other sharp peaks were found in this work.

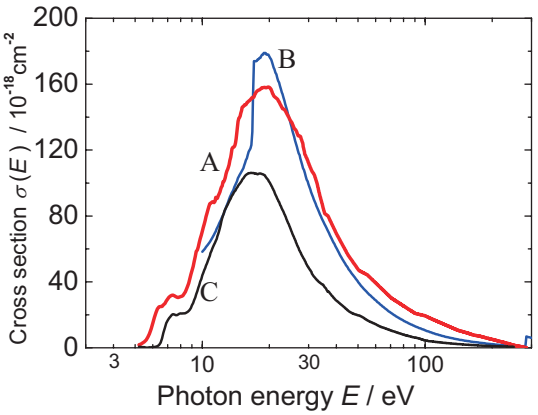

Fig. 1. Absorption cross section spectra $\sigma(E)$ of L-alanyl-L-alanine obtained by experiment (curve A) and by calculation (curve B). Curve C is $\sigma(E)$ of L-alanine reported by Kamohara *et al*. [2].

This work is supported by the Use-of-UVSOR Facility program (2011, 23-817, 23-819, 23-824) of the Institute for Molecular Science.

*Present address: JASRI/SPring-8.

[1] J. O. Hirschfelder, C. F. Curtiss, R. B. Bird, 1954. Molecular Theory of Gases and Liquids. Wiley, New York, p. 890.
[2] M. Kamohara, Rad. Phys. Chem. **77** (2008) 1153.
[3] http://henke.lbl.gov/optical_constants/

BL6U

Ultrafast Molecular Dissociation as a Tool for Dissociative Potential Energy Surface Mapping

R. Guillemin[1], M. N. Piancastelli[1], M. Simon[1], H. Iwayama[2] and E. Shigemasa[2]
[1]*LCPMR, Université Pierre et Marie Curie, 75231 Paris Cedex 05, France*
[2]*UVSOR Facility, Institute for Molecular Science, Okazaki 444-8585, Japan*

In quantum mechanics, potential energy surfaces (PES) are a representation of the structural and dynamical properties of molecular systems. As such, they are essential tool to describe and predict chemical properties and chemical reactivity.

The motivation behind this study is to provide an experimental determination of PES, i.e. the change of potential energy with the inter-atomic distance. A way to achieve this is to perturb the system in such a way that it will respond by a change in geometry, and monitor the spectral variation while the electronic wave packet explores the PES. It was suggested that this could be achieved by electron core excitation and radiative decay monitoring [1]. Recently, it was shown that in the case of bond states, vibrational core excitation provides a way to map PES efficiently [2].

Here, we take advantage of ultrafast dissociation following C 1s core excitation in CF_4 [3] and ultrahigh resolution measurements of the subsequent Auger decay to explore dissociative PES.

The experiment was performed on the soft X-ray beamline BL6U at UVSOR. The radiation from an undulator was monochromatized by a variable included angle varied line-spacing plane grazing monochromator. The photon energy resolution E/ΔE was set to 5000. The monochromatized radiation was introduced into a cell with sample gases. Kinetic energies of the emitted electrons were measured by a hemispherical electron energy analyzer (MBS-A1) placed at a right angle with respect to the photon beam direction. The degree of the linear polarization of the incident light was essentially 100%, and the direction of the electric vector was set to be parallel to the axis of the electrostatic lens of the analyzer. The kinetic energy resolution of the analyzer was set to 60 meV.

Figure 1 (top) shows the absorption spectrum of CF_4 around the $\sigma^*(t_2)$ resonance below the C 1s ionization threshold, and the 2D map of the associated Auger decay spectrum in the region of the participator decay (bottom) as a function of photon energy. The spectrum shows dispersive lines that correspond to the direct photoionization of the valence states of CF_4. These lines are overlapping with the resonant Auger decay of the molecule that can be revealed by subtracting at each photon energy, the direct photoionization lines, as shown in Fig. 2. Two features in this spectrum reveal the dynamics of ultrafast dissociation of the molecule.

On the high-energy side, a non-dispersive electron emission is interpreted as the decay from the core-excited CF_3^* dissociated fragment.

On the low-energy side, the dispersive electron emission shows a large asymmetric tail that reveals the elongation of the C-F bond in competition with the Auger decay. The change of kinetic energy in this dynamical Auger emission correlates directly to the potential energy difference between the PES of the intermediate core-excited state and the PES of the final dissociated ionic state, effectively mapping the PES. Theoretical analysis of the experimental data is underway.

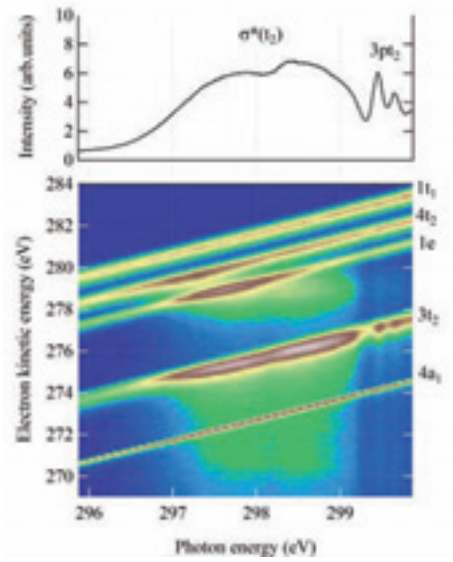

Fig. 1. Full decay spectrum measured at the $\sigma^*(t_2)$ resonance of CF_4.

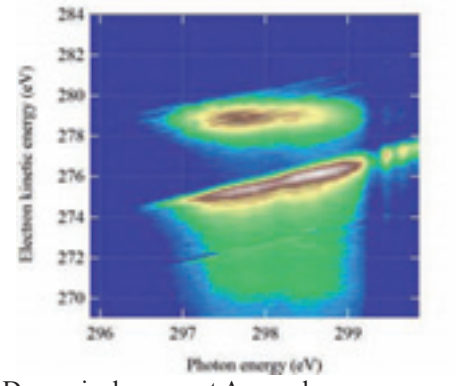

Fig. 2. Dynamical resonant Auger decay.

[1] S. Carniato *et al.*, Chem. Phys. Lett. **439** (2007) 402.
[2] C. Miron *et al.*, Nature Phys. **8** (2011) 135.
[3] K. Ueda *et al.*, Phys. Rev. Lett. **83** (1999) 3800.

BL6U

Ultrafast Molecular Dissociation of Core-Excited HBr Studied by High-Resolution Electron Spectroscopy

E. Shigemasa[1], H. Iwayama[1], K. Soejima[2] and P. Lablanquie[3]
[1]*UVSOR Facility, Institute for Molecular Science, Okazaki 444-8585, Japan*
[2]*Department of Enviromental Science, Niigata University, Niigata 950-2181, Japan*
[3]*LCPMR, Université Pierre et Marie Curie, 75231 Paris Cedex 05, France*

Soft X-ray absorption spectra of molecules exhibit rich structures in the region below the ionization thresholds, which are due to the excitations of a core electron to unoccupied valence or Rydberg orbitals. The core excited states are predominantly relaxed via Auger electron emission, in the case of the molecules composed of light elements, and subsequently fragmentation follows. As demonstrated by Morin and Nenner, however, a fast neutral dissociation could precede the resonant Auger decay [1]. In other words, the electronic decay of the core hole takes place after the constituent atoms come apart. Since then, many research works have been conducted to identify such ultrafast dissociation processes in various different systems. Recent works on high-resolution resonant Auger electron spectroscopy have revealed that the nuclear motion of the molecular core-excited states is promoted in competition with the Auger decay. Here, we revisit the first discovery of ultrafast dissociation following the Br 3d core excitation in HBr [1]. High-resolution electron spectroscopy for the subsequent Auger decay has been applied.

The experiments were carried out on the soft X-ray beamline BL6U at UVSOR. The radiation from an undulator was monochromatized by a variable included angle varied line-spacing plane grazing monochromator. The exit slit opening was set to 300 μm, which corresponds to the photon energy resolution E/ΔE of ~1500 at 70 eV. The monochromatized radiation was introduced into a gas cell with sample gases. Kinetic energies of the emitted electrons were measured by a hemispherical electron energy analyzer (MBS-A1) placed at a right angle relative to the photon beam direction. The degree of the linear polarization of the incident light was essentially 100%, and the direction of the electric vector was set to be parallel to the axis of the electrostatic lens of the analyzer. The energy resolution of the analyzer was set to ~12 meV. Under these experimental conditions, the full width at half maximum of the vibrational fine structure for the X state of HBr^+ was measured to be ~50 meV.

Figure 1 shows the total ion yield spectrum of HBr in the vicinity of the Br 3d ionization threshold. The broad feature centered at around 71 eV is assigned to the 3d → σ* resonance, which has two components $3d_{5/2}$, $3d_{3/2}$ of the initial core hole states. Figure 2 represents a resonant Auger spectrum taken at 70.4 eV, where the $3d_{5/2}$ core-hole states are mainly populated. The vertical scale of the red line spectrum is magnified by the five times. The most marked feature in Fig. 2 is the numerous sharp peaks, due to the vibrational structures for the HBr^+ states and the atomic Auger lines from the Br fragments with a 3d core-hole. In the previous work [1], only five atomic lines indicated by the blue arrows in Fig. 2 have been identified, owing to the limited resolution. In contrast, at least ten more atomic Auger peaks and some molecular peaks with vibrational structures are clearly resolved in the present work. The detailed analyses for the spectral features observed are just beginning to be performed.

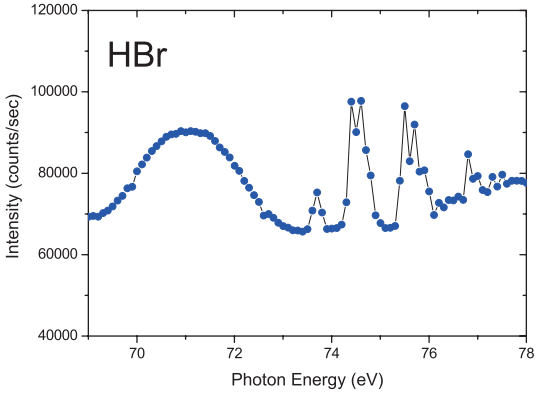

Fig. 1. Total-ion yield spectrum (E/ΔE ~1500) in the Br 3d excitation region of HBr.

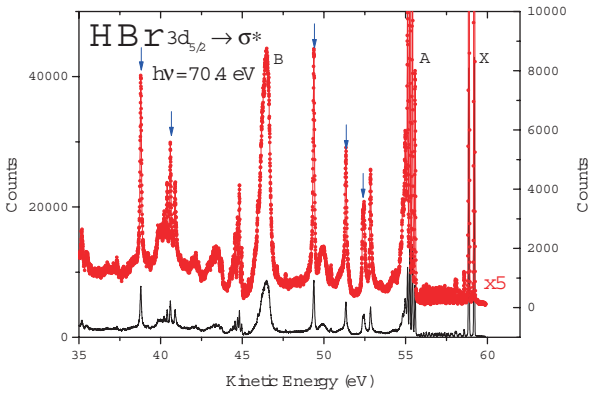

Fig. 2. Resonant Auger spectrum taken at the Br $3d_{5/2}$ → σ* resonance.

[1] P. Morin and I. Nenner, Phys. Rev. Lett. **56** (1986) 1913.

BL6U

Double Auger Decays after 3d Core Ionization or Excitation in HBr Studied by High-Resolution Electron Spectroscopy

P. Lablanquie[1], H. Iwayama[2], K. Soejima[3] and E. Shigemasa[2]
[1]*LCPMR, Université Pierre et Marie Curie, 75231 Paris Cedex 05, France*
[2]*UVSOR Facility, Institute for Molecular Science, Okazaki 444-8585, Japan*
[3]*Department of Environmental Science, Niigata University, Niigata 950-2181, Japan*

Shallow inner shell holes such as 3d in Kr usually decay by emission of a single Auger electron. However, with a probability of ~10%, two Auger electrons can also be released, mainly sequentially [1]. In the HBr isoelectronic molecule, it was found that the molecule can dissociate during this sequential emission of Auger electrons [2]. More precisely, the first emitted Auger electron e_{A1} populates an HBr^{2+} state that dissociates before the second Auger electron e_{A2} is emitted from the Br^{+*} fragment:

$$HBr^{+}(3d^{-1}) \rightarrow HBr^{2+} + e_{A1} \rightarrow H^{+} + Br^{+*}$$
$$\text{followed by: } Br^{+*} \rightarrow Br^{2+} + e_{A2}$$

In this study, we have used a high resolution electron analyser to examine in fine detail these secondary 'atomic' Auger electrons e_{A2}.

The experiments were carried out on the soft X-ray beamline BL6U. The radiation from an undulator was monochromatized by a variable included angle varied line-spacing plane grazing monochromator. The monochromatized radiation was introduced into a gas cell with sample gases. Kinetic energies of the emitted electrons were measured by a hemispherical electron energy analyzer (MBS-A1) placed at a right angle relative to the photon beam direction. The degree of linear polarization of the incident light was essentially 100%, and the direction of the electric vector was set to be parallel to the analyzer axis.

Figure 1 compares the high resolution electron spectrum (in blue) obtained here above the 3d ionization threshold at hν = 90 eV, with the one of reference [2] (red). The latter implied the coincident detection of the associated 3d photoelectron and e_{A1} Auger electron, thus providing an unambiguous identification of the process. It is seen that the present non coincident measurement probes the same process but with a much higher resolution, and demonstrates clearly that the atomic decay involves autoionization of two Rydberg series of Br^{+*} $4p^4(^2D_J)nl$ configurations (with J = 3/2 or 5/2) to the Br^{2+} (^4S) ground state.

Figure 2 shows that the same atomic lines appear also upon excitation of the 3d → σ* resonance. This resonance is well known for the associated ultrafast dissociation producing H and Br* $3d^{-1}4s^24p^6$ fragments. Single Auger decay of this Br* fragment is well documented (see associated Activity Report); the present results demonstrate that double Auger decay of the Br* fragment also occurs.

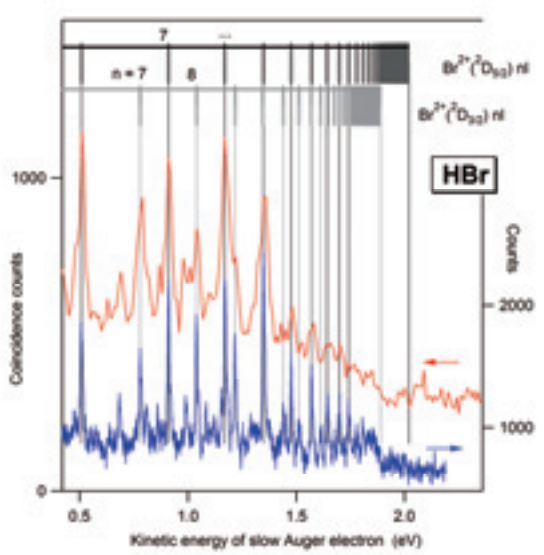

Fig. 1. (blue) High resolution spectrum of low energy electrons measured at hν = 90 eV, and compared to the lower resolution one from reference [2] (red). The energy resolution of the analyzer was set to ~5 meV.

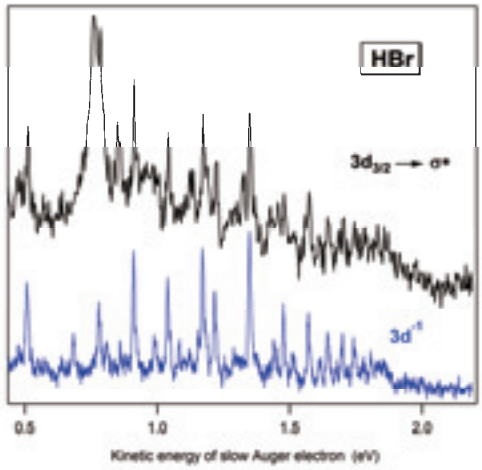

Fig. 2. Comparison of the high resolution electron spectra measured above the 3d threshold (blue, as in Fig. 1) and on the $3d_{3/2} \rightarrow \sigma^*$ resonance at hν = 72 eV.

[1] J. Palaudoux *et al.*, Phys. Rev. A **82** (2010) 043419.
[2] F. Penent *et al.*, Phys. Rev. Lett. **106** (2011) 103002.

BL6U

Doppler Effect in Fragment Autoionization Following Core-to-Valence Excitation of OCS

H. Iwayama and E. Shigemasa
UVSOR Facility, Institute for Molecular Science, Okazaki 444-8585, Japan

When the source and observer are in motion relative to each other, the Doppler effect is known to occur, leading to an apparent change in the observed frequency of the propagating wave. This effect has a wide variety of applications in many fields, relating to the sensing of movement. Since Gel´mukhanov and co-workers predicted in 1997 [1] that the nuclear motion in 'ultrafast dissociation' following molecular core-level photoexcitation can be probed by the Doppler effects in emitted Auger electron, many research works have been conducted. Ultrafast dissociation is a process in which the molecular dissociation at the core-excited state precedes the Auger decay and then an atomic fragment emits an Auger electron [2]. The atomic Auger electron can possess the opposite Doppler shift depending on the direction approaching the detector or moving away from it.

Recently, the electronic Doppler effects after the core-to-Rydberg excitations in N_2 and the core-to-valence excitations in O_2 have been revealed [3,4]. In the present work, experiments for observing the electronic Doppler effects in atomic Auger-electron emissions from S fragments have been performed in the S 2p excitation region of OCS.

The experiment was performed on the soft X-ray beamline BL6U. The radiation from an undulator was monochromatized by a variable included angle varied line-spacing plane grazing monochromator. The photon energy resolution E/ΔE was set to 1000. The monochromatized radiation was introduced into a cell with sample gases. Kinetic energies of the emitted electrons were measured by a hemispherical electron energy analyzer (MBS-A1) placed at a right angle with respect to the photon beam direction. The degree of the linear polarization of the incident light was essentially 100%, and the direction of the electric vector was set to be either parallel or perpendicular to the axis of the electrostatic lens of the analyzer. The kinetic energy resolution of the analyzer was set to 12 meV.

Figure 1 represents the blowup of an atomic Auger line following the ultrafast dissociation [2] in the resonant Auger spectrum obtained at 165.5 eV, where the S $2p_{1/2} \rightarrow \pi^*$ and S $2p_{3/2} \rightarrow \sigma^*$ resonances lie. The observed atomic Auger line clearly demonstrates the Doppler profile, depending on the polarization direction. On the basis of the symmetry-resolved photoion yield spectra [5], the photoion anisotropy parameter β at 165.5 eV can be estimated to be about -0.29. Assuming that the axial recoil approximation is well valid, and the lifetime broadening and instrumental resolution are equal to 65 and 12 meV, respectively, the kinetic energy release in the present study is determined to be about 1.7 eV. The detailed data analysis is now in progress.

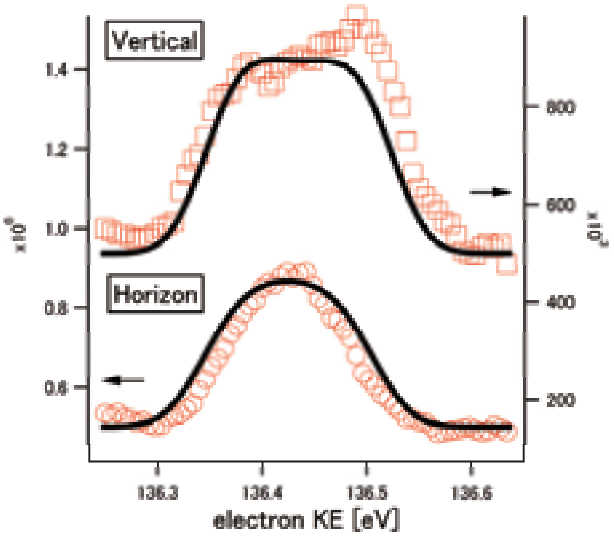

Fig. 1. Doppler profile of atomic Auger line measured at the S $2p_{1/2} \rightarrow \pi^*$ and S $2p_{3/2} \rightarrow \sigma^*$ resonance position of OCS. Solid circles and solid squares in red are experimental data points measured at horizontal and vertical polarization, respectively. Solid lines denote the fitting results.

[1] F. Gel´mukhanov, H. Ågren and P. Sałek, Phys. Rev. A **57** (1998) 2511.
[2] P. Morin and I. Nenner, Phys. Rev. Lett. **56** (1986)1913.
[3] E. Shigemasa *et al.*, New J. Phys. **12** (2010) 063030.
[4] R. Guillemin *et al.*, Phys. Rev. A **82** (2010) 051401(R).
[5] S. Masuda, T. Hatsui and N. Kosugi, J. Electron Spectrosc. Relat. Phenom. **137-140** (2004) 351.

BL6U

Ultrafast Dissociation of Core-Excited OCS Studied by Two Dimensional Electron Spectroscopy and Electron–Ion Coincidence Spectroscopy

L. Ishikawa, H. Iwayama and E. Shigemasa
UVSOR Facility, Institute for Molecular Science, Okazaki 444-8585, Japan

Coincidence detection and correlation analysis among the particles ejected during the relaxation processes of core-excited molecules bring a deeper insight into the molecular inner-shell processes. When both an Auger electron and fragment ions are analyzed in energy, one can give access to the state-to-state dissociation dynamics of the core-excited molecules. In the previous work [1], the correlation between the resonant Auger electrons with their biding energy ranging from 14.5 to 19 eV and subsequent molecular dissociation following the S $2p_{3/2} \rightarrow \pi^*$ excitation of OCS molecules has been investigated. Here, we take advantage of ultrafast dissociation processes following the S 2p core excitations in OCS. Auger-electron–ion coincidence spectroscopy as well as high-resolution 2 dimensional (2D) electron spectroscopy has been applied.

The experiments were carried out on the soft X-ray beamline BL6U. For the 2D electron spectroscopy, the monochromator bandwidth was set to $E/\Delta E$ ~1000 at $h\nu$=165eV. Kinetic energies of the emitted electrons were measured by a hemispherical electron energy analyzer (MBS-A1) placed at a right angle relative to the photon beam direction. The direction of the electric vector was set to be either parallel or perpendicular to the axis of the electrostatic lens of the analyzer. The resonant Auger spectra with kinetic energies ranging from 135 to 155 eV were recorded as a function of the photon energy in the S 2p excitation region.

For the coincidence experiment, the monochromator bandwidth was set to $E/\Delta E$ ~10000 at $h\nu$=165eV. The electrons ejected at 54.7° relative to the electric vector of the light were analyzed in energy by the double toroidal electron analyzer (DTA), while ions were extracted from the interaction region into the momentum spectrometer by a pulsed electric field according to the electron detection. The pass energy of the DTA was set to 100 eV for observing resonant Auger electrons in a binding energy range from 29 to 31 eV. It has been confirmed in the separate experiment that there is a sharp peak due to the atomic Auger line from the core excited S atoms in the corresponding energy region. The coincidence data set was recorded at $h\nu$=165.5 eV, which corresponds to the S $2p_{1/2} \rightarrow \pi^*$ and S $2p_{3/2} \rightarrow \sigma^*$ excitations.

Figure 1 shows the 2D map of resonant Auger electron spectra following the S 2p excitation of OCS measured in horizontal direction. The diagonal lines in Fig. 1 are due to the valence photoelectrons, while the vertical lines seen in the lower kinetic energy region are owing to the atomic Auger lines. The atomic line widths show clear polarization dependence, which may reflect the anisotropic photoexcitation process. According to the symmetry-resolved photoion yield spectra [2], the photoion anisotropy parameter β at 165.5 eV is estimated to be about -0.29. Figure 2 represents the angular distribution of the S^+ ions taken in coincidence with the atomic Auger line. The β value of -0.24 estimated through a fitting procedure is in reasonably good agreement with the above value. This means that the initial molecular orientation induced by photoexcitation is kept in the present case.

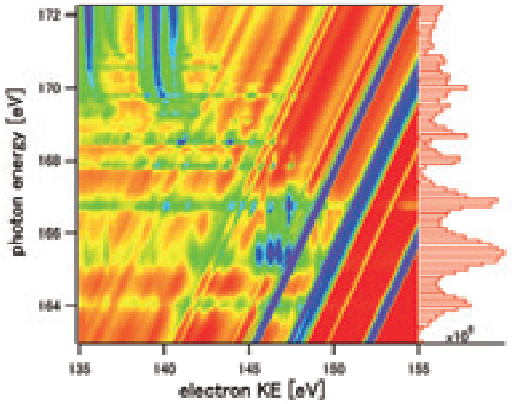

Fig. 1. 2D map of resonant Auger electron spectra following the S 2p excitation of OCS.

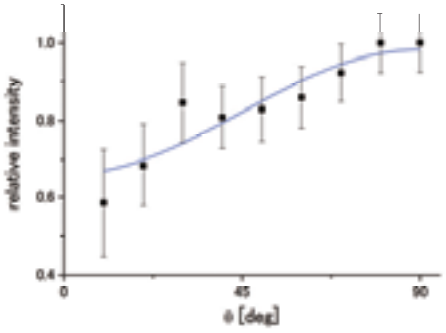

Fig. 2. Angular distributions of S^+ ions taken in coincidence with the atomic Auger electrons.

[1] T. Kaneyasu, M. Ito, Y. Hikosaka and E. Shigemasa, UVSOR Activity Report **34** (2007) 59.
[2] S. Masuda, T. Hatsui and N. Kosugi, J. Electron Spectrosc. Relat. Phenom. **137-140** (2004) 351.